IEEE Access
Multidisciplinary ⋮ Rapid Review ⋮ Open Access Journal

Received April 12, 2022, accepted April 27, 2022, date of publication May 3, 2022, date of current version May 11, 2022.

Digital Object Identifier 10.1109/ACCESS.2022.3172322

Reduced Simulative Performance Analysis of Variable Step Size ANN Based MPPT Techniques for Partially Shaded Solar PV Systems

SHAIK RAFI KIRAN[1], C. H. HUSSAIAN BASHA[2], VISHWA PRATAP SINGH[3], C. DHANAMJAYULU[4], (Senior Member, IEEE), B. RAJANARAYAN PRUSTY[4], (Senior Member, IEEE), AND BASEEM KHAN[5], (Senior Member, IEEE)

[1]Department of Electrical and Electronics Engineering, Sri Venkateswara Engineering College, Tirupati, Andhra Pradesh 517502, India
[2]Department of Electrical Engineering, Nanasaheb Mahadik College of Engineering, Walwa, Maharashtra 415407, India
[3]Department of Computer Science Engineering, Guru Gobind Singh Indraprastha University, Dwarka, Delhi 110078, India
[4]School of Electrical Engineering, Vellore Institute of Technology, Vellore, Tamilnadu 632014, India
[5]Department of Electrical and Computer Engineering, Hawassa University, Hawassa 6240, Ethiopia

Corresponding authors: C. Dhanamjayulu (dhanamjayulu.c@vit.ac.in) and Baseem Khan (baseem.khan04@gmail.com)

ABSTRACT The rise in energy demand in the present scenario can be balanced with the help of solar Photovoltaic (PV) systems. But, the nonlinearity in I-V and P-V characteristics makes it very difficult to extract the maximum power of the solar PV. Also, the classical Maximum Power Point Tracking (MPPT) techniques fail to track the global Maximum Power Point (MPP) from the multiple local MPPs under Partial Shading Conditions (PSCs). In this work, a Variable Step Size ANN-based MPPT technique is proposed and it is compared with the other MPPT techniques in terms of steady-state behavior, settling time of converter power, power point tracing speed, oscillations of MPP, and operating efficiency. The compared MPPT techniques are Adaptive Perturb & Observe (AP&O), Adaptive Feed Forward Neural Network Controller (AFFNNC), Artificial Neural Network-based P&O (ANN-based P&O), ANN-based Incremental Conductance (ANN-based IC), ANN-based Hill Climb (ANN-based HC), and Radial Basis Functional Controller based Fuzzy (RBFC based Fuzzy). The boost converter is interfaced in the middle of the PV system and load to step-up the PV supply voltage. The performance of selected neural networks MPPT techniques is studied by utilizing a MATLAB/Simulink window.

INDEX TERMS ANN, boost converter, duty cycle, efficiency, high tracing speed of MPP, less oscillations, less convergence time, less settling time.

NOMENCLATURE

Symbols	*Parameters*	*Values*
P_{MPP}	Peak extracted power at MPP	250.0 W
V_{MPP}	Peak available voltage at MPP	30.01 V
I_{MPP}	Peak available current at MPP	8.302 A
N_{pp}	Total strings working parallel	1.0
N_{ss}	Available series modules in one string	3.0
N_s	One module available cells	60.0
r_s	PV cell resistance in series	0.3102 Ω
r_p	Resistance of cell in parallel	313.298 Ω
V_{oc}	PV cell voltage at OC	36.80 V
I_{sc-n}	PV cell current at SC	8.829 A
I_{0-n}	Diode current at saturation condition	$1.023*\exp 10^{-10}$A
T_n	Working standard temperature	25^0C
G_n	Irradiations of sun at nominal condition	1000 W/m^2

The associate editor coordinating the review of this manuscript and approving it for publication was Yongming Li.

K_v	Voltage coefficient at T_n	-0.301 %/deg. C
K_i	Current coefficient at T_n	0.059 %/deg. C
a_1, a_2, and a_3	Diode ideality factors	0.89, 0.92, and 1
T	Basic working temperature of PV	45^0C

I. INTRODUCTION

To the recent global energy survey, renewable energy systems are the most popular power distribution systems because of their properties are low greenhouse gas emissions, high reliability, more flexibility, cheap generation cost, and high efficiency when associated with the conventional source-based power generating systems [1]. The major classifications of renewable energy sources are wind, tidal, solar, and fuel cell. The wind source is available free of cost, and this type of wind plant is installed near the hilly areas. The wind blades absorb the natural wind force and it transfers the force from the wind blades to the generator side. The rotor of the generator rotates until the availability of kinetic energy of wind. The disadvantages of wind systems are less continuity in supply, and less reliability [2]. So, most of the current researchers are working on solar-related power generation, and distribution systems. The generation of each PV cell voltage is 0.7V which is very negligible [3]. So, plenty of cells are interfaced with each another to enhance their supply voltage rating. The cells are interfaced in a parallel way to improve the load current rating.

The PV cells are designed by utilizing several fabricating technologies which are illustrated as mono, plus polycrystalline technologies. The working efficiency of ploy and thin film-based PV cells is less when equated to the monocrystalline [4]. From the literature study, the PV cells are availed in various forms which are one diode equivalent type, double diode equivalent circuit model, and triple diode equivalent model. Among all of these diode models, the most utilized one is the triple diode model-based solar PV cell [5]. In this work, the triple diode model-related solar PV cell is considered for the analysis of a PV-fed non-isolated power converter system. The advantages of triple diode circuit type solar PV cell are good working efficiency, high utilization factor, and more extracted output voltage when associated with the other PV cell topologies.

The PV systems are implemented by interfacing the triple diode type circuit model solar strings and the PV array generates nonlinear power versus voltage characteristics. So, the finding of Maximum Power Point (MPP) is a very problematic task. From the previously published works, there are several types of MPPT methods are available in the market. The most frequently studied MPPT techniques are classical, metaheuristic, artificial intelligence, and soft computing optimizing techniques [6].

The classification of classical power point finding techniques are Perturb & Observe (P and O), Incremental Resistance (IR), fractional voltage, and fractional current controllers. Also, the hill climb controller is utilized where the oscillations of MPP are very high. In article [7], a P and O concept is used for the perturbation of the I-V curve step value. The perturbation value consists of a plus indication then only it varies in a similar direction or else, the perturbation goes in the opposite direction. The demerits of the P&O technique are more fluctuations of the working point of solar PV and less convergence speed. The IR method is proposed in an article [8] for continuous efficiency enhancement of hybrid solar PV grid interfaced systems. In this technique, the current density is considered for finding the slope of the P-V characteristics. The only limit of the IR technique is high design complexity.

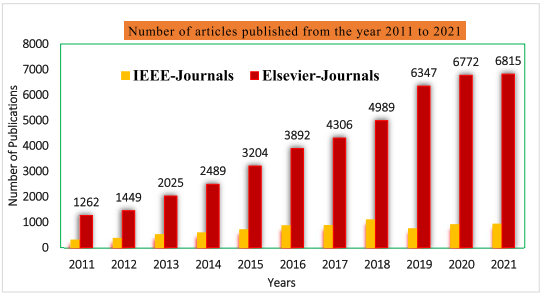

FIGURE 1. Graphical representation of MPPT articles publications [12].

So, the limitations of the IR controller are compensated by using the fractional-based current MPPT controller.

In this controller, the short circuit current of PV is determined by separating the triple diode PV circuit from the power converter. Also, this type of MPPT technique is useful for less accurate traffic signal applications [9]. The drawback of the short circuit current MPPT technique is its tracing speed which is purely dependent on the selection of the PV system. The detailed MPPT-related articles publication is illustrated in Figure.1. As of Figure.1, it is represented that maximum power point finding controllers are applied in most of the PV and wind hybrid power supply systems. The classification of power point-defining controllers is given in Figure.2.

In the open circuit-based voltage MPPT technique, the MPP is identified by using a separate switch in the PV interfaced power converter [10]. So, the overall controller implementation cost, and size are increased. Every converter generates solar PV ripple voltage and current. The generated electrical signals are supplied to the Kalman filter block for filtering the ripple content of the converter power, and obtaining the required duty pulses to the single switch power converter-based hybrid power generation network [11]. The features of the Kalman filter method are optimum in size, acceptable accuracy, and quick response when compared to the other classical MPPT controllers.

In article [12], a feedback controller is proposed for rising the output solar power distribution network. The selected supply parameters for this feedback block are changes in

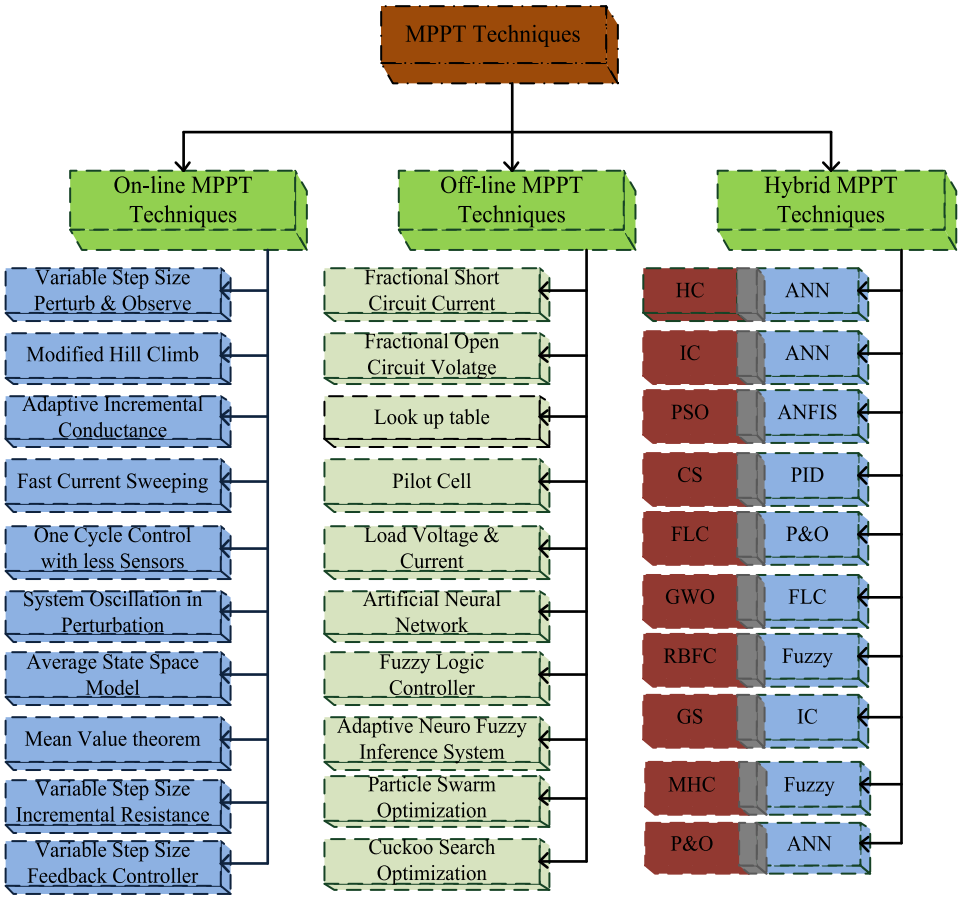

FIGURE 2. **Classification of power point finding techniques.**

voltage and power. The corresponding output parameter of the feedback controller is the maximum voltage error signal. However, the classical–controllers are unable to find out the exact MPP position of PV at various shading conditions [13]. So, in this article, a radial basis function controller-dependent fuzzy controller is proposed for finding the accurate MPP position with few oscillations. The features of this proposed hybrid controller are less dependency on PV array modeling, low steady-state settling time, and quick convergence speed.

The solar PV systems supply very less output voltage which may not be sufficient for the high voltage gain electric vehicle applications. So, the researchers are using the dc-dc power converters for improving the voltage profile of the sunlight-dependent PV systems [14]. As from the previously published works, the power converters are differentiated as transformer-dependent boost converters and transformerless boost converters. In article [15], the authors utilized the transformer involved power converters for high frequency rated automotive applications. This type of power converter consists of additional rectifiers for transforming the alternating current to direct supply. Also, these transformer-dependent converters give floating output power concerning the input. The merits of isolated converters are high safety from the overvoltage's, breaking of all ground loops, level shifting, and high voltage gain [16]. But, the major demerit is more expensive.

The forward isolated converter is interfaced in the micro grid-based solar power system for improving the working efficiency of the PV module. This type of converter consists of a high voltage rating transformer which is double the input voltage. Here, the active snubber circuit concept is utilized for resets the transformer core every time. The drawbacks of the forward-type converter are high operating conduction losses, and more in size [17]. The demerits of the forward isolated converter are limited by using the flyback converter. The limits of the flyback converter are operating at less leakage inductor current, pulsating supply current, and moderate working efficiency [18]. The disadvantages of the flyback converter are compensated by using the isolated Cuk converter [19]. The isolated Cuk converter is utilized in permanent magnet synchronous generator fed solar PV systems for enhancing the power factor, and voltage regulation of the electrical machine. Also, this converter is compared with the isolated zeta converter under various conduction modes of operations. From the analysis, it has been identified that the isolated converter topologies required a high design cost. So, in this work, a non-isolated DC-DC power converter is used for enhancing the voltage gain of the PV module. The

features of the converter are easy design, high flexibility, less implementation cost, and more reliable.

II. LITERATURE SURVEY ON MPPT TECHNIQUES

An adaptive IC MPPT technique is proposed in the article [20] to track the peak power based on the slopes of I-V and P-V characteristics of solar PV at different irradiation conditions. The slope of the I-V curve will be zero, positive or negative based on the position of the operating point is at the true peak point, on left or on the right side of the PV curve respectively. This technique also takes more time to track the true peak power. Unlike the conventional techniques, as the name suggests current sweeping MPPT technique purely depends on PV current to track the maximum power [21]. The tracking speed of this technique is moderate under different Partial Shading Conditions (PSCs) and is dependent on the time constant of solar PV.

The tracking speed of the PV is improved by applying one cycle control technique, this method does not require any phase-locked loop controller to interface the inverter and grid. This technique is highly reliable, rugged, and cost-effective [22]. But, this method gives moderate power point convergence speed. From the current literature history, most manufacturers, and research scholars are developing the artificial neural network-related MPPT controller. In article [23], an ANN correlated power point finding controller is investigated for high output power rated PV systems to resolve the nonlinearity issue. The working behavior of the neural network is pretty identical to the biological neuron. The disadvantages of neural power point identifying controllers are high data training time and moderate accuracy.

So, the neural controller is combined with the classical precise linearization-based state feedback MPPT technique for increasing the working performance of boost converter-related PV fed induction machine systems [24]. The merits of a state feedback controller are the possibility of reducing the state transient error in the system, acceptable accuracy, and enhanced robustness from external disturbances. Also, this method gives proper reliability, and repeatable value. The only demerit is continuous changes in the output response.

In article [25], the authors utilized the Incremental Conductance grounded neural network system for the grid-connected inverter integrated hybrid solar and wind power distribution system. Here, the multiple layer neural controller has been utilized for finding the approximation-dependent MPP position. Later, the variable conductance technique is used for minimizing the variation of the functioning point of the solar PV. Also, the authors tested the proposed ANN-based IC method by considering the field-programmable dependent gate array vertex-II. However, this hybrid methodology gives low convergence speed, and high implementation difficulty. In addition that this type of controller is less suitable for shaded conditions of PV systems.

The fuzzy power point finding controller is applied in the article [26] for increasing the voltage value of the solar PV-based buck-boost converter. The fuzzy system gives superior performance when equated to the neural network [27]. Here, the controller commands are initiated based on the variation of voltage, and current across the PV module. The most considerable features of fuzzy systems are highly robust and don't require any precise input signals. But, the fuzzy logic-related power point identifying controllers gives unsatisfied accuracy. The high-performance related soft computing MPPT techniques are discussed in the article [28] for extracting the peak power of the PV array. Usually, the fuzzy is an outer performance of other power point identifying controllers in nonlinear, complex, and approximated structures for which the most user-friendly knowledge exists.

Under the shaded condition of the solar PV module, the finding of operating peak power point is very difficult.

The fuzzy controller is combined with the improved GWO technique to improve the accuracy, very low oscillations of MPP, and less dependency on the type of PV array selected. Also, this hybrid technique gives high efficiency of PV in various atmospheric temperature situations [29]. In article [30], the authors proposed the genetic algorithm optimized neural controller for standalone solar PV-based induction machine drive system to optimize the duty of the buck-boost converter. Here, the induction drive is directly coupled with the supply device. The main objective of the genetic algorithm is to find a total number of neurons in the multilayer feed-forward artificial neural network. The merits of this hybrid controller are moderate complexity in structure, ideal in size, and highly adaptable for continuous variation of solar irradiation conditions. Also, it helps the power converter to work at less output power losses.

In article [31], the authors utilized the beta parameter-dependent fuzzy controller for dc-dc converter interfaced solar PV system. Here, the beta variable selects the optimum number of fuzzy rules. In this MPPT controller, the authors considered the three input variables which are PV voltage, beta, and PV current. The output of this hybrid controller is the change of duty value. The hybrid power generation system is selected in the article [32] for optimizing the size of the battery-operated vehicles. The battery integrated PV systems design cost is very high. The cost of the system is minimized by interfacing the bat algorithm-based fuzzy system. The input and output variables of fuzzy systems are-initiated with the help of the Bat technique. Also, the bat algorithm selects the appropriate membership functions for the corresponding supply and output variables of the fuzzy controller.

III. ANALYSIS OF PARTIALLY SHADED SOLAR PV SYSTEM

As we discussed previously, the PV array modeling has been done by selecting a triple diode circuit-based solar PV cell. Here, the number of cells is interconnected for improving the solar irradiation incident area [33]. The parameters required for the design of a triple diode circuit based PV cell are short circuit current (I_{SC}), ideality factors (a_1, a_2, and a_3), the peak voltage of PV (V_{MPP}), open-circuit voltage (V_{oc}), and peak to

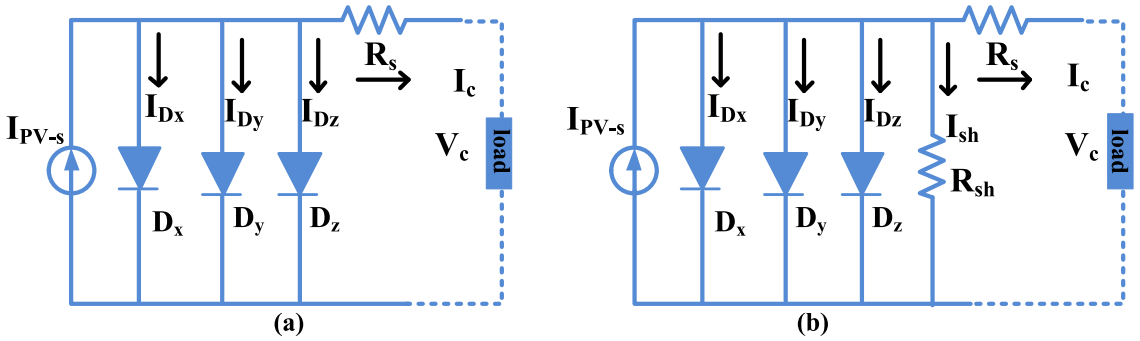

FIGURE 3. Triple diode circuit solar PV cell, (a) without shunt resistance and (b) with shunt resistance.

peak current (I_{MPP}). The graphical representation of a triple diode-based solar PV cell without shunt resistance, and with shunt resistance are given in Figure.3 (a), and 3(b). From Figure.3 (a), the solar PV current is derived as,

$$I_0 = I_{PV\_s} - I_{D_x} - I_{D_y} - I_{D_z} \tag{1}$$

$$I_c = I_{PV\_s} - i_{revs\_1}(e^{\frac{q(V_c+I_c*R_s)}{\eta_1 KT}} - 1) - I_x \tag{2}$$

$$I_x = i_{revs\_2}(e^{\frac{q*(V_c+I_cR_s)}{\eta_2 KT}} - 1) + i_{revs\_3}(e^{\frac{q*(V_c+I_cR_s)}{\eta_3 KT}} - 1) \tag{3}$$

$$I_{PV\_s} = (I_{PV\_sSTC} + K_i\Delta T) * \frac{G}{G_{STC}} \tag{4}$$

$$I_c = I_{PV\_s} - i_{revs\_1}\left(e^{\frac{q(V_c+I_c*R_s)}{\eta_1 KT*n_s}} - 1\right) - I_x \tag{5}$$

$$I_x = i_{revs\_2}\left(e^{\frac{q*(V_c+I_cR_s)}{\eta_2 KT*n_s}} - 1\right) + i_{revs\_3}\left(e^{\frac{q*(V_c+I_cR_s)}{\eta_3 KT*n_s}} - 1\right) \tag{6}$$

From Fig.3 (b), the solar PV cell involved both parallel, and series resistances then the PV current is derived as,

$$I_c = I_{PV\_s} - I_{Dx} - I_{Dy} - I_{Dz} - I_{sh} \tag{7}$$

$$I_c = I_{PV\_s} - i_{revs\_1}\left(e^{\frac{q(V_c+I_cR_s)}{\eta_1 KT}} - 1\right) - i_{revs\_2}\left(e^{\frac{q(V_c+I_cR_s)}{\eta_2 KT}} - 1\right) - I_y \tag{8}$$

$$I_z = i_{orev\_3}\left(e^{\frac{q(V_c+I_cR_s)}{\eta_3 KT}} - 1\right) + \frac{V_c + I_cR_s}{R_{sh}} \tag{9}$$

$$I_{revs\_1} = I_{revs\_2} = I_{revs\_3} = I_{on}(\frac{T}{T_N})^3 e^{\frac{qE_g}{nk}\left(\frac{1}{T_N} - \frac{1}{T}\right)} \tag{10}$$

$$I_{on} = I_{on\_1} = I_{on\_2} = I_{on\_3} = \frac{I_{SC\_n}}{e^{\left(\frac{V_{oc\_n}}{\eta V_{Tn}}\right)}} \tag{11}$$

Most solar power plants are installed near rooftops and hilly areas. So, the shading effect exists on solar PV modules due to the clouds, building shadows, and trees falling. Under constant irradiation value, the number of peak power points that exist on P-V characteristics is one. Similarly, at shading conditions, the existed peak power points on solar nonlinear characteristics are multiple and are classified as local MPPs and global peak power point. The required global peak power point is tracked by utilizing soft computing techniques instead of classical MPPT controllers.

The shaded solar PV modules under various incident irradiations are shown in Fig.4. As of from Figure.4 (a), the incident irradiations on all three PV modules are equal to 1000W/m2. In Figure.4 (b), (c), plus (d), the PV modules are coming to the shading condition. At the time of shading condition, the corresponding PV modules bypass diodes are comes to the ON condition, and the remaining unshaded PV modules bypass diodes are in the OFF state. Here, the unshaded PV supply power is consumed by the shaded PV modules and their transfer to the heat losses. The nonlinear curves of PV under shading behavior are shown in Fig.5 (a), and 5(b). From Fig.5 (b), it has been indicated that there are two local MPP positions (^{x1}, and y1), and single global required position (g) at every shaded condition.

At constant irradiation conditions, the extracted peak voltage, and power are calculated as 92.25V, and 750W. The maximum extracted PV power, and corresponding voltage at 1000 W/^{m2}, 890 W/m2, and 690W/m2 are determined as 574W, and 92.01V. Similarly, at 1000 W/m2, 790 W/^{m2}, and 690W/^{m2}, the obtained peak voltage, and peak power are 91.52V, plus 550.45W respectively. In this proposed solar PV system, there are two major types of power losses are occurred at the time of partially shaded solar PV systems which are misleading power loss, and mismatch power loss. The solar modules are misleading, and mismatch power losses are determined as 7.2W, and 178.21W respectively.

IV. DESIGN OF MPPT TECHNIQUES AT VARIOUS PSC'S

In shaded conditions, the PV modules may give very less supply power. As a result, the supply system may not reach the load demand. Moreover, the system working heat conduction losses are increased. Another major factor of solar PV is its design and implementation cost which is minimized by using the various power point finding techniques [34]. From the above literature review, it has been stated that conventional power point determines controllers may not give a fast response when equated to artificial intelligence controllers. In this article, a VSS-RBFC-dependent fuzzy logic

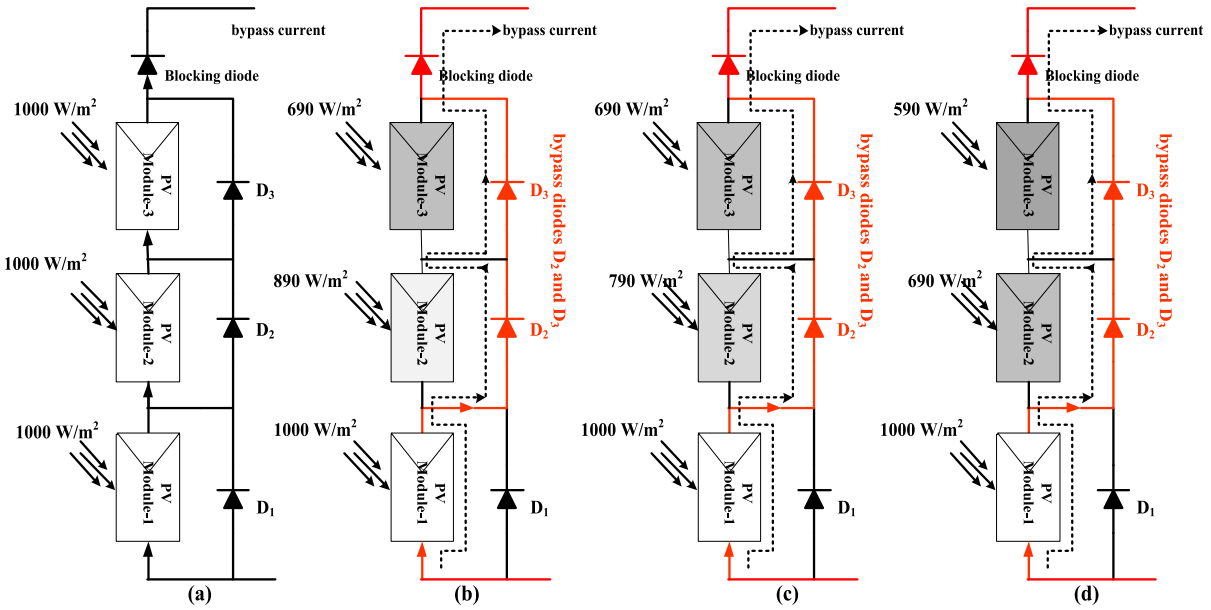

FIGURE 4. Shaded behavior of solar PV modules, (a) 1000 W/m^2, 1000 W/m^2, plus 1000 W/m^2, (b) 1000 W/m^2, 890 W/m^2, plus 690 W/m^2, (c) 1000 W/m^2, 790 W/m^2, plus 690 W/m^2, and (d) 1000 W/m^2, 690 W/m^2, plus 590 W/m^2.

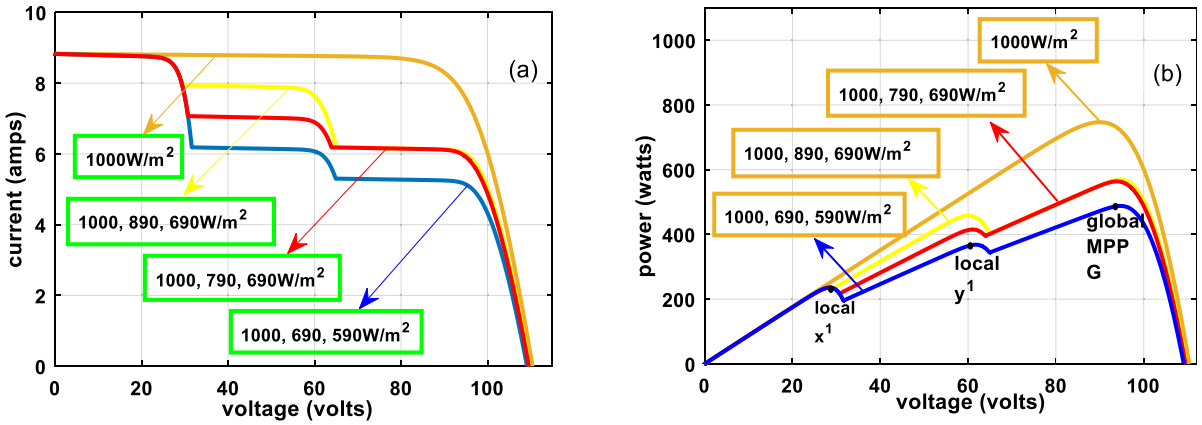

FIGURE 5. Solar PV, (a) I–V curves and (b) P–V curves at various shaded conditions.

controller is proposed for fast and accurate tracking of MPP position. Here, the proposed controller is compared with the other existing hybrid artificial intelligence controllers such as AP&O, AFFNNC, ANN-based IC, and ANN-based HC controllers.

A. ADAPTIVE VSS-P&O MPPT CONTROLLER

The general P&O controller is utilized in various low power rating solar power generation systems and it's the most common controller in most automotive applications. But, the demerits of this controller at shading behavior of PV are unable to find out the required peak voltage of PV. Also, this controller gives more distorted grid voltages [35]. Here, an advanced adaptive P&O method is applied to the standalone power supplying system for automatic adjustment of the step length of the solar PV nonlinear curve. The working diagram of adaptive conventional P&O dependent controller is represented in Fig.6. Based on Fig.6, it is seen that the adaptive MPPT technique increased the duty value of the classical converter when the functioning point of PV is placed at the left corner I-V curve. Otherwise, the working duty value of the power converter is reduced step by step when the functioning point of PV is on the right-hand side of the I-V curve. The converter duty adjustment is illustrated in Eq. (12), and (13).

$$D(x) = D(x-1) + \gamma * \left(\frac{p(x) - p(x-1)}{v(x) - v(x-1)}\right) \quad (12)$$

$$D(x) = D(x-1) - \gamma * \left(\frac{p(x) - p(x-1)}{v(x) - v(x-1)}\right) \quad (13)$$

B. FEED FORWARD NEURAL NETWORK MPPT CONTROLLER

As of now, the neural networks are implemented and designed from the biological process of natural neurons. Neural

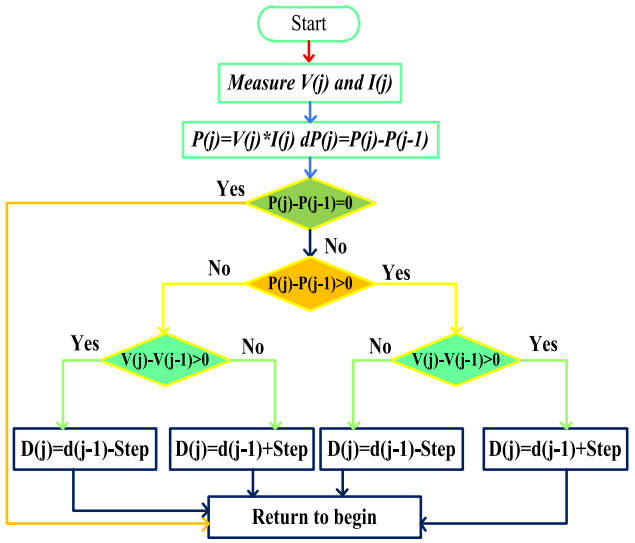

FIGURE 6. Working flow of adaptive related P&O power point finding controller.

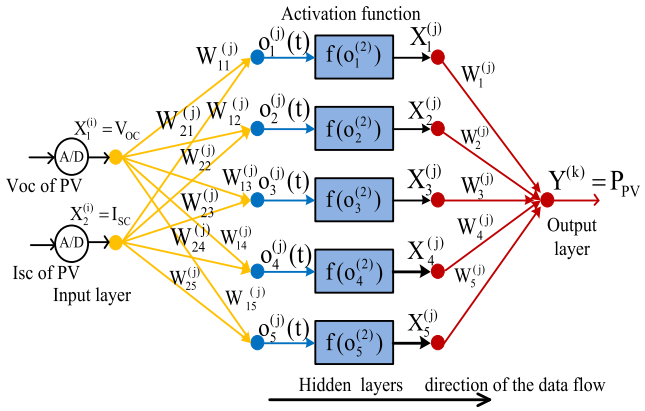

FIGURE 7. Feed forward artificial intelligence MPPT Controller.

networks are computer programming-related networks that are interconnected with each another. The neuron is represented as a node, and the overall combination of nodes forms a layer. In article [36], a feed-forward neural controller is utilized for the solar system to limit the shading power loss. The architecture of this MPPT controller involved three layers which are named as the supply input layer, the hidden layer, plus the output generated layer. The training of a feed-forward neural network has been done by utilizing the back-propagation concept. The representation of FFNN is illustrated in Fig.7. From Fig.7, the selected parameters for this neural network are short-circuited current and open circuit-based voltage. The output required signal from the network is solar PV power that can be compared with the actual available power. The obtained error signal from the neural network is fed to the proportional plus integral controller. The first-order PI controller optimizes the steady-state, plus transient error. So that the entire system power quality is improved. The middle, and output layers of neural network controllers' input, plus output signals are obtained which are given in below Eq's.

$$o_a^{(2)}(t) = \sum_{b=1}^{2} W_{ab}^{(2)} * L_b^1; a = 1, 2, 3 \ldots\ldots, 9 \quad (14)$$

$$L_a^{(2)}(t) = f\left(o_a^{(2)}(t)\right) \quad (15)$$

$$N^3(t) = \sum_{b=1}^{5} W_b^{(3)} * L_b^{(2)} \quad (16)$$

$$W_{ab}^{(2)} = W_{ab}^{(2)} + \Delta W_{ab} \quad (17)$$

$$W_b^{(3)} = W_{b3}^{(3)} + \Delta W_b \quad (18)$$

$$\Delta W_{ab} = u * \frac{\partial e}{\partial W_{ab}^{(2)}},$$

$$+ \Delta W_b = u * \frac{\partial e}{\partial W_b^{(3)}} \quad (19)$$

$$e = \frac{1}{2}(P_{desired} - P^{(3)})^2 \quad (20)$$

C. ARTIFICIAL NEURAL NETWORK ASSOCIATED P&O MPPT CONTROLLER

The basic artificial intelligence controllers may not give the needed power point of the PV. In article [37], the parameter considered for processing the multilayer neural system is peak solar PV voltage. The supervised learning methodology is utilized in this neural system for obtaining an accurate training response. Also, the supervised methodology is useful for the mapping between the supply variables and related output variables. In this method, the neural controller works based on the solar parameters such as PV voltage, diode ideality factors, open circuit-related voltage, and atmospheric temperature. In this hybrid NN-based P&O controller, at the–initial stage, the neural architecture is utilized to move the functioning point of PV near to the required working point. However, there are few oscillations near the MPP position that can be limited by utilizing the P&O controller as shown in Figure.8. From Fig.8, the P&O controller compares the actual power error value to the present power value. Based on the comparative results, the controller starts working in the forward direction, or else, it moves in the reverse direction. The merits of this controller are high tracing MPP speed, and suitable for high power standalone solar PV applications.

D. ARTIFICIAL NEURAL NETWORK-BASED IC MPPT CONTROLLER

The incremental conductance of the I-V is considered for moving the functioning point of PV near to the actual working point. The conductance of PV is consist of a positive indication when the functioning point of PV left side of the solar PV nonlinear curve. Sometimes, the functioning point of PV is on the right side of the nonlinear curve then the conductance of PV consists of a negative indication. The merits of IC are easy understanding, simplicity in design, high convergence speed, less design cost, and popularity. However, the drawbacks of IC are moderate power oscillations near the MPP, and high complexity when associated with the conventional P&O controller. Due to that, the hybrid ANN-based IC controller is

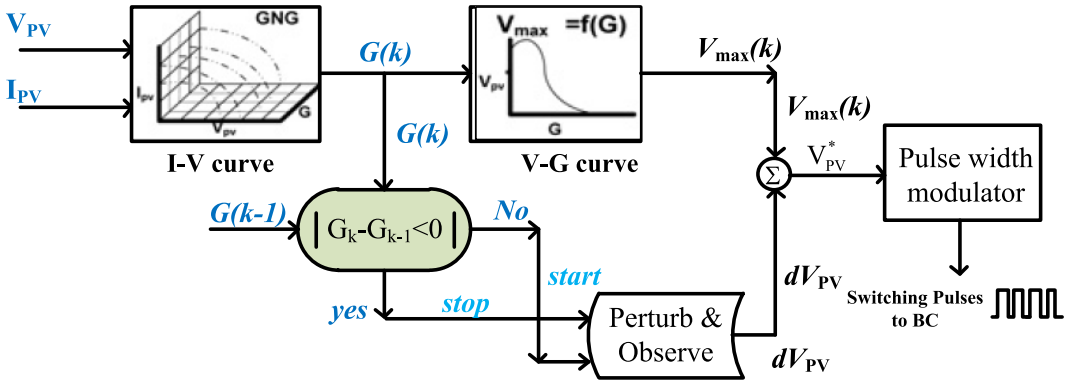

FIGURE 8. Artificial intelligence dependent P&O associated MPPT controller.

utilized in the article [38] for enhancing the working behavior of solar PV. Here, the duty value updating of IC is derived as,

$$D(i) = D(i-1) + D_{step} \times \text{sig}\left(\frac{\Delta I}{\Delta V} + \frac{I}{V}\right) \quad (21)$$

$$D(i) = D(i-1) - D_{step} \times \text{sig}\left(\frac{\Delta I}{\Delta V} + \frac{I}{V}\right) \quad (22)$$

$$D_{step} = \tau \frac{\Delta P}{\Delta V}; \lambda = \frac{\Delta P}{\Delta V} \quad (23)$$

From Eq. (21), the term "D (i), & D (i-1)" are defined as instant and past duties of the power converter. Also, the term "D_{step}" is identified as the variation of step-change on the P-V curve.

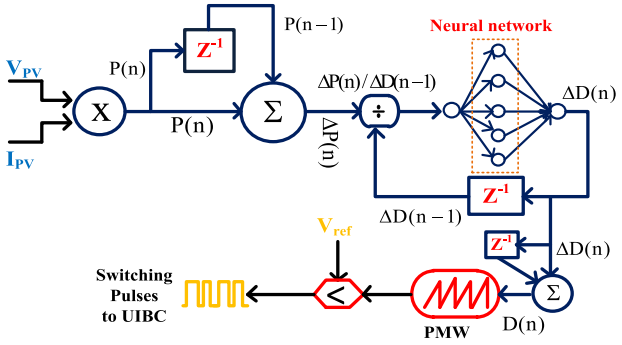

FIGURE 9. Hill climb correlated neural network MPPT controller.

E. ARTIFICIAL NEURAL NETWORK-BASED HC MPPT CONTROLLER

From the literature work, the classical power point-defining controllers are combined with artificial intelligence concepts for enriching the functioning point of solar PV near the actual peak voltage point. Here, in the article [39], the hill climb technique is combined with an artificial intelligence controller for developing the hybrid low-cost MPPT controller. As from the previous discussion, the P&O technique can produce high continuous oscillations across MPP. Moreover, it may not be applicable for shaded-type solar power production systems. So, the limitations of this basic controller are adjusted by projecting a hill climb controller. The combination of a hill climb with an artificial neural network controller is shown in Fig.9. Based on Fig.9, at starting, the neural network starts working to fast up the tracking speed of maximum power point. The neural controller selects the proper input variables to find out the required duty value of a conventional power converter. Here, the variation power related to the time is illustrated clearly.

F. PROPOSED VSS-RBFC BASED FUZZY LOGIC CONTROLLER

As of from the literature review, the studied classical power identifying controllers may trace the local functioning point of PV instead of the global working point. The basic conventional neural controller requires efficient knowledge–person on statically analysis, and calculus. Additionally, these controllers require more training and storage data. The neural architectures are formed from the multiple layers of interconnected neurons. The biological neurons may be represented as the nodes. The data transformation or process has been done from the supply layer to the required output layer. Similarly, the multilayer related power point finding controller involves multiple numbers of hidden layers. Due to that, the neural-dependent system implementation complexity has been improved. Additionally, the multilayer controller computational time is very high.

So, in the article [40], the authors proposed the soft computing associated fuzzy logic controller for tracing continuous variation of MPP of solar PV. The fuzzy has the capability of solving engineering-based uncertainty issues and can give accurate solutions to complex nonlinear problems. However, this fuzzy power point finding controllers may not be applicable for the partially shaded solar PV systems. So, in this article, a variable step dependent radial basis functional controller associated fuzzy is introduced. Here, the merits of fuzzy, and ANN are considered for implementing the hybrid power point finding controller. In this hybrid MPPT controller, at starting, a variable step RBFC is utilized for adjusting the functioning point of the PV array near the required power point location position. Later, a fuzzy controller is

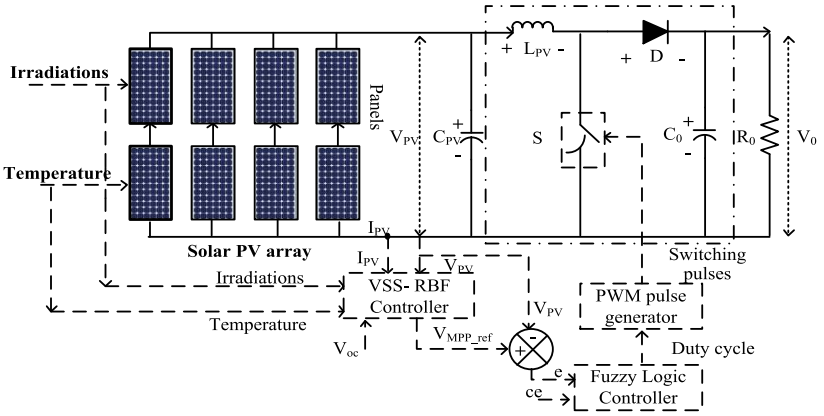

FIGURE 10. Proposed solar PV system with hybrid MPPT controller.

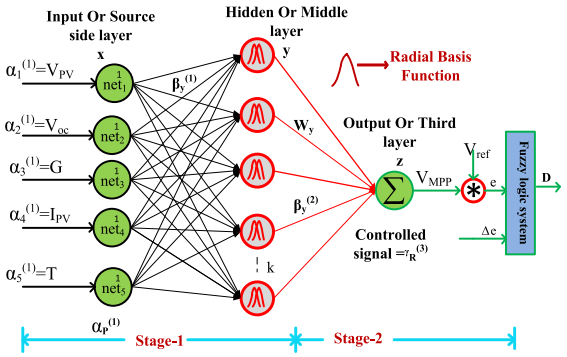

FIGURE 11. Proposed hybrid RBFC associated fuzzy logic MPPT controller.

utilized for handling the changes in MPP position as shown in Figure.10.

From Fig.10, the network is trained by utilizing the two types of learning methods which are classified as supervised, plus unsupervised techniques. The supervising concept is used at the input side layer for giving the initial weights to the neural nodes. After that, the unsupervised methodology is applied to run the RBF controller, and the weights of neural layers are updated with the help of this learning algorithm. Here, the continuous variation of solar insolation, operating temperature of the sun, open-circuit voltage, maximum peak current, and voltages are given to the input to the RBF controller as shown in Fig.11. From Fig.11, the RBF is quite similar to the feed-forward neural network. The main differences are the selection of activation function, the total number of neurons, and the number of hidden layers. The present utilized RBF consists of five input neurons, nine hidden layer nodes, and one output side node. The net, and outputs of input, hidden, and output layers are derived as,

$$\beta_x^1(k) = f_x^1 net_x^1(k) = net_1^1(k); k = 1, 2..n \quad (24)$$

$$net_y^2(k) = -(i - m_y)^T \sum_y (i - m_y); k = 1.2.., n \quad (25)$$

$$\beta_y^2(k) = f_y^2 net_y^2(k) = net_y^2(k); k = 1.2.., n \quad (26)$$

TABLE 1. Fuzzy logic controller-based MPPT technique rules.

e \ *ce*	NB	NM	NS	ZO	PS	PM	PB
NB	NB	NB	NB	NB	NM	NS	ZE
NM	NB	NB	NB	NM	NS	ZE	PS
NS	NB	NB	NM	NS	ZE	PS	PM
ZE	NB	NM	NS	ZE	PS	PM	PB
PS	NM	NS	ZE	PS	PN	PB	PB
PM	NS	ZE	PS	PM	PB	PB	PB
PB	ZE	PS	PM	PB	PB	PB	PB

$$net_z^3 = \sum_y W_y * \beta_z^2(k); k = 1.2 \ldots .., n \quad (27)$$

$$\beta_z^3(k) = f_z^3 net_z^3(k) = net_z^3(k); k = 1.2 \ldots, n \quad (28)$$

$$error = \sum_{k=1}^{\alpha} \frac{1}{2} (V_{ref} - V_{MPP}) \quad (29)$$

From Eq. (24), the term‘’ is represented as an overall neuron in the proposed RBFC network. The standard deviation of every layer is selected as ‘$_{my}$’. The summation term from Eq. (25) is selected as Σ which represents the Gaussian mean of the system. Here, in the RBFC network, every node of the hidden layer works as an individual membership value. The term‘’ represents the maximum peak voltage of PV which is determined by the linear activation of the network. The output-generated signal is fed to the fuzzy system. The error and change of error of peak voltage of PV are processed by using the fuzzification block. The fuzzy converts the set of real value data into a crisp solution. The available crisp values are fed to the inference block for producing the if-then concept. At last, the processed crisp variables are transferred to real variables by utilizing the defuzzification system. Here, the fuzzy logic controller membership functions are shown in Fig.12, and their corresponding rules are given in Table.1. The fuzzy controller received the error, and variations of error parameters are derived as,

$$e(y) = V_{MPP}^*(y) - V(y) \quad (30)$$

$$ce(y) = e(y) - e(y - 1) \quad (31)$$

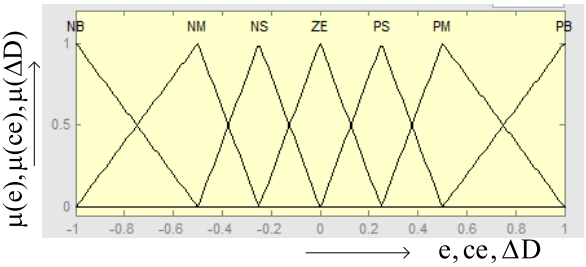

FIGURE 12. Fuzzy logic controller based duty cycle for PSC solar PV system.

V. ANALYSIS AND DISCUSSION OF SIMULATION RESULTS

The major consideration of PV is its nonlinear current versus voltage characteristics. Also, under the shaded condition of PV, the nonlinear curves are having multiple maximum power points. So, the conventional or classical MPPT techniques may not be suitable for the diverse atmospheric temperature, and irradiation values. Here, the analysis of various power point finding controllers has been done by applying the hybrid artificial intelligence MPPT techniques. The features of hybrid artificial neural networks are fast tracing speed, required very few sensors for sensing the PV parameters, fast convergence speed, and very less fluctuations of MPP when equated with the classical MPPT techniques. The classical converter converts the low PV output voltage to high PV output voltage.

The classical converter consists of one input side capacitor ($C_{PV} = 10\mu F$), plus one output side capacitor ($C_0 = 0.55mF$). The input capacitor is most useful for the suppression of PV voltage fluctuations. Also, it gives the constant PV output power for the power converter system. Similarly, the load side capacitor is helpful for the constant load demand application. Moreover, this capacitor helps protect the devices from overload voltages. The inductor (L_{PV} =1.247mH) is utilized for smoothing the solar PV current and it supplies ripple-free current to the load. The merits of this converter are continuous output voltage, and more voltage conversion ratio when equated to the other classical converters.

A. SOLAR PV AT PSC-1 (1000W/M2, 890W/M2, PLUS 690W/M^2)

Here, all the artificial intelligence-based MPPT techniques are studied by applying MATLAB software. The selected MPPT method's comparative performance has been done in terms of oscillations, error at steady state, design complexity, and operating efficiency at three various partial shaded solar power supply systems. The PV modules received irradiations at initial shaded conditions are 1000W/m2, 890W/m2, plus 690W/m2. The solar PV, and converter output voltage, current, and power waveforms are illustrated in Fig.13. From Fig.13 (a), the adaptive P&O, multilayer feed-forward neural network, and ANN-based power tracking controllers help the solar PV to extract the extreme peak current. Based on Fig.13 (b), the produced voltages and powers of PV by employing the ANN-based P&O, ANN-based HC, ANN-based IC, and RBFC based Fuzzy controllers are 91.654V, 561.716W, 91.89V, 562.577W, 91.721V, and 562.003W respectively.

The settling times of PV-generated voltages by utilizing adaptive P&O, and AFFNNC are 0.351, and 0.318. From Fig.13(d), (e), plus (f), it is identified that the RBFC based Fuzzy controller gives very less converter output power, current, and voltage waveforms distortions. The detailed performance investigation of various power point identifying controllers for solar power fed power converter are given in Table.2. Based on the recorded parameters of the solar PV system, the operating duty cycle of the power converter from the utilization of adaptive P&O is 0.75 which is more when equated with the ANN-based HC controller. Moreover, the adaptive P&O controller takes more time for finding the MPP position. So, the classical power point finding controller is less applicable for the PV shaded conditions.

B. SOLAR PV AT PSC-2 (1000W/M2, 790W/M2, PLUS 690W/M^2)

Here, the available three PV modules strings are shaded by observing the irradiations are 1000W/m2, 790W/m2, and 690W/m2. The shaded PV module's power extraction has been done by applying the conventional as well as soft computing MPPT controllers. The generated DC-link voltages of the power converter by utilizing the Adaptive P&O, Adaptive FFNNC, plus ANN-based P&O controllers are 89.931W, 90.896W, and 90.997W.

The obtained PV modules currents, plus voltages by utilizing the various artificial intelligence controllers are defined in Figure.14 (a), and (b). Also, the converter working duty cycle by employing the classical MPPT methods is illustrated in Figure.14(c). Based on Figure.14(c), the power converter receives the optimum required duty value from the RBFC based fuzzy logic MPPT controller. The obtained power converter generated current, and power waveforms are shown in Figure.14 (e), and (d).

The shaded solar PV modules give the high MPP tracing time by utilizing the adaptive feed-forward artificial intelligence controller when associated with the artificial intelligence-dependent IC controller. The received currents of PV from the application of adaptive P&O, ANN-based HC, and RBFC based Fuzzy controller are 5.9635A, 5.915A, and 5.9A respectively. So, it can be seen that the available current of PV by the application of RBFC based fuzzy logic controller is less. As a result, the entire PV system power delivering losses are less when equated with the other nonconventional MPPT methods. The steady-state settling times of converter-generated power from the utilization of AFFNNC, and adaptive P&O are 0.328sec, and 0.358sec respectively. The analysis of various MPPT controllers for shaded PV power supply DC-DC converter is given in Table.3. From Table.3, it can be observed that the converter-generated voltage waveforms consist of heavy

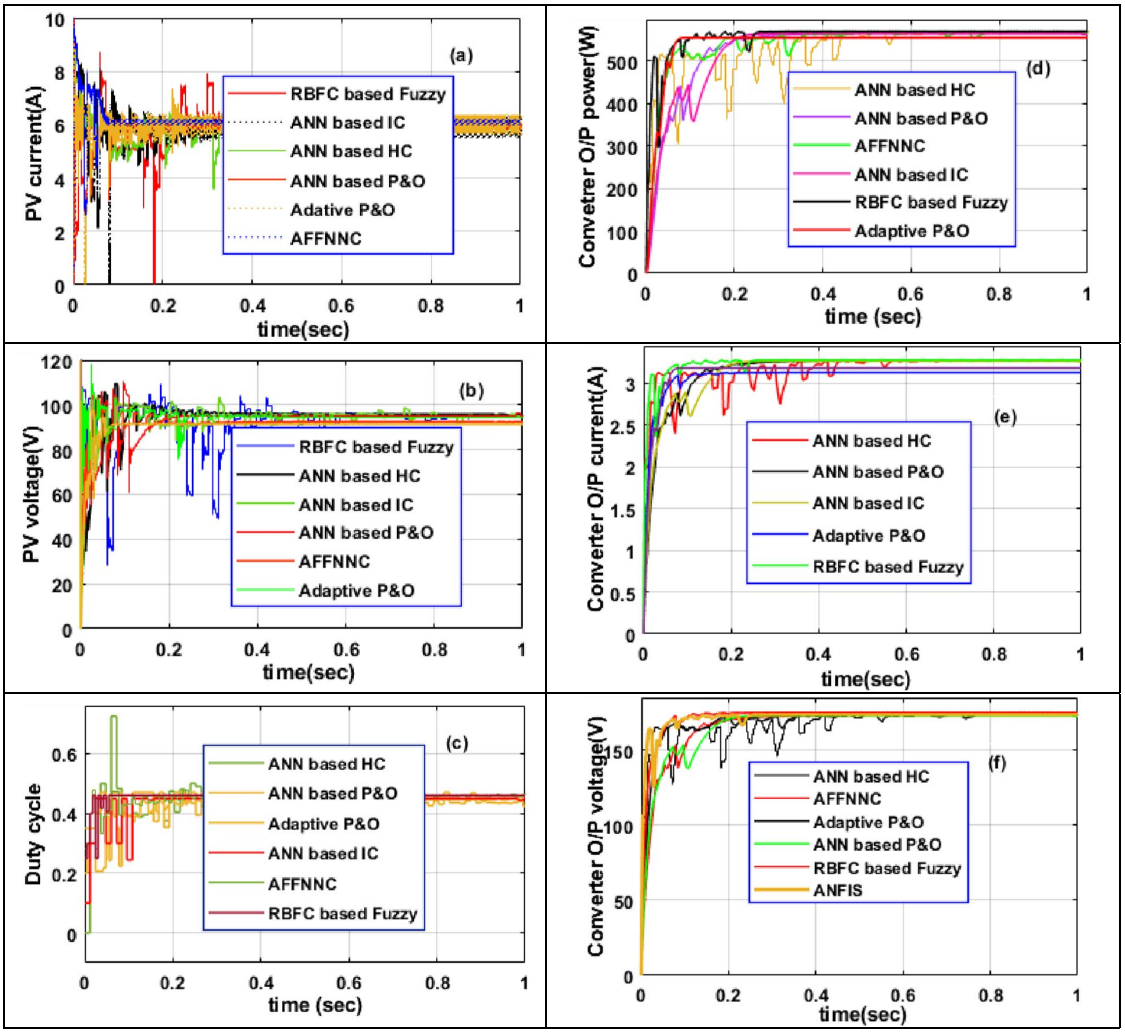

FIGURE 13. (a). Solar PV generated current, (b) solar voltage, (c) duty cycle, (d) converter generated power, (e) converter generated current, and (f) a voltage of converter at PSC-1.

TABLE 2. Simulative analysis of ANN-based power point finding techniques at 1000, 890, plus 690W/m ^{2}.

Parameters	Adaptive P&O	Adaptive FFNNC	ANN-based P&O	ANN-based IC	ANN-based HC	RBFC based Fuzzy
Dc-link capacitor voltage	91.228	91.50	91.654	91.721	91.890	92.0
PV current (A)	6.135	6.133	6.128	6.127	6.1222	6.12
PV power (W)	559.724	561.211	561.716	562.003	562.577	563.782
Global Power (W)	574	574	574	574	574	574
Tracking efficiency (%)	97.513	97.772	97.860	97.91	98.01	98.22
State settling time(sec)	0.351	0.318	0.303	0.326	0.293	0.250
Distortion in waveforms	High	Moderate	Moderate	High	Less	Less
Tracking speed (sec)	0.317	0.285	0.281	0.218	0.220	0.198
Duty cycle	0.750	0.741	0.72	0.612	0.59	0.53

distortions by the application of AFFNNC when equated with the ANN-based HC. Moreover, the working duty of the power converter from the utilization of ANN-based P&O is 0.792. Finally, the converter voltage is high by the utilization of RBFC based fuzzy controller which is illustrated in Figure.14 (f). So, at the shaded condition of PV, the artificial intelligence-related MPPT controllers give more accurate response.

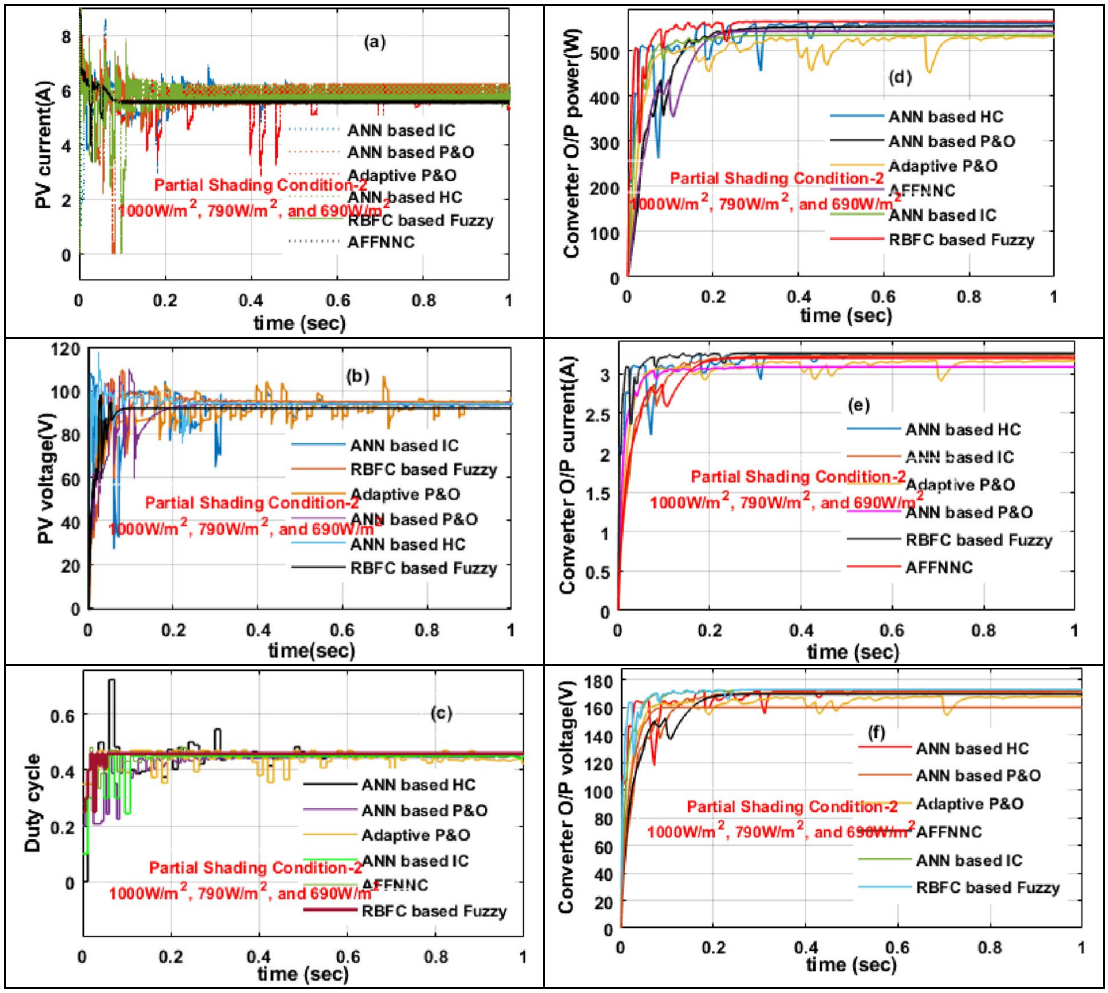

FIGURE 14. (a). Solar PV generated current, (b) solar voltage, (c) duty cycle, (d) converter generated power, (e) converter generated current, and (f) voltage of converter at PSC-2.

TABLE 3. Simulative analysis of ANN-based power point finding techniques at 1000, 790, plus 690W/m^2.

Parameters	Adaptive P&O	Adaptive FFNNC	ANN-based P&O	ANN-based IC	ANN-based HC	RBFC based Fuzzy
Dc-link capacitor voltage	89.931	90.896	90.997	91.052	91.180	91.52
PV current (A)	5.9635	5.9015	5.9129	5.9154	5.915	5.90
PV power (W)	536.31	536.424	538.064	538.615	539.385	540.266
Global Power (W)	550.45	550.45	550.45	550.45	550.45	550.45
Tracking efficiency (%)	97.433	97.452	97.750	97.85	97.99	98.15
Steady state settling time(sec)	0.358	0.328	0.305	0.302	0.300	0.252
Distortion in waveforms	High	Moderate	Moderate	High	Less	Less
Tracking speed (sec)	0.321	0.292	0.293	0.304	0.228	0.2.0
Duty cycle	0.760	0.751	0.792	0.618	0.602	0.56

C. SOLAR PV AT PSC-3 (1000W/M2, 790W/M2, PLUS 690W/M^2)

The obtained current and PV voltage of the sun-dependent power generation system are shown in Fig.15 (a), and (b). The available DC-link voltages from the application of artificial related P&O, adaptive FFNNC, and neural network dependent fuzzy systems are 89.931V, 90.896V, and 91.52V respectively. Similarly, the PV power system operated duty values from the application of artificial intelligence-based IC, and HC are 0.618, and 0.605 which is illustrated in Fig.15(c). The obtained power of PV by utilizing the RBFC dependent fuzzy power point finding technique is 540.266 and its working related efficiency is 98.15%. Similarly, the tracking speed of this RBFC

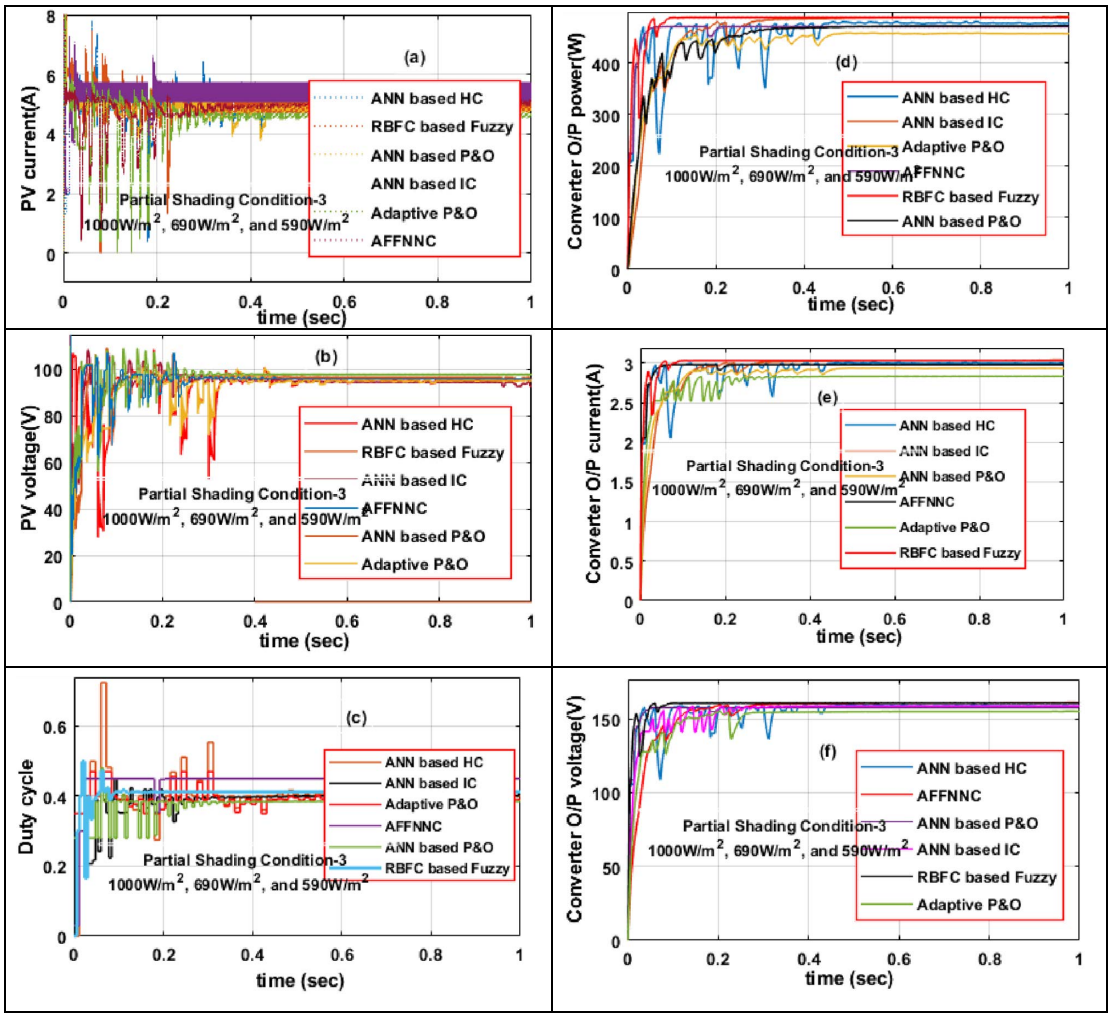

FIGURE 15. (a). Solar PV generated current, (b) solar voltage, (c) duty cycle, (d) converter generated power, (e) converter generated current, and (f) voltage of converter at PSC-3.

TABLE 4. Simulative analysis of ANN-based power point finding techniques at 1000, 790, plus 690W/m^2.

Parameters	Adaptive P&O	Adaptive FFNNC	ANN-based P&O	ANN-based IC	ANN-based HC	RBFC based Fuzzy
Dc-link capacitor voltage	89.931	90.896	90.997	91.052	91.180	91.52
PV current (A)	5.9635	5.9015	5.9129	5.9154	5.915	5.90
PV power (W)	536.31	536.424	538.064	538.615	539.385	540.266
Global Power (W)	550.45	550.45	550.45	550.45	550.45	550.45
Tracking efficiency (%)	97.433	97.452	97.750	97.85	97.99	98.15
Steady state settling time(sec)	0.358	0.328	0.305	0.302	0.300	0.252
Distortion in waveforms	High	Moderate	Moderate	High	Less	Less
Tracking speed (sec)	0.326	0.302	0.298	0.238	0.234	0.206
Duty cycle	0.770	0.7642	0.798	0.618	0.605	0.610

controller is very high when equated with the other MPPT controllers. The converter obtained power waveforms, current waveforms, and voltage waveforms are explained in Figure.15 (d), (e), plus (f). Based on Figure.15 (d), it can be seen that the RBFC controller extracts high peak power with few steady-state distortions near the actual MPP. The analyzed parameters of MPPT techniques are shown in Table.4.

VI. CONCLUSION

The proposed RBFC based fuzzy logic controller dependent MPPT controller is designed by utilizing the MATLAB/Simulink environment. The proposed MPPT technique is equated with the other conventional, artificial intelligence-based MPPT techniques in terms of settling time of MPP, distortions in obtained converter generated power, MPP finding efficiency, number of sensing variables, power transfer losses, and PV module dependency. Based on the performance results, it has been identified that the RBFC optimized Fuzzy controller helps the solar power converter to work with high efficiency in various partially shaded situations. Also, it has been determined that the conventional power point identifying controllers are less suitable for PSCs

REFERENCES

[1] N. Afsharzade, A. Papzan, M. Ashjaee, S. Delangizan, S. Van Passel, and H. Azadi, "Renewable energy development in rural areas of Iran," *Renew. Sustain. Energy Rev.*, vol. 65, pp. 743–755, Nov. 2016.

[2] J. Shair, X. Xie, L. Wang, W. Liu, J. He, and H. Liu, "Overview of emerging subsynchronous oscillations in practical wind power systems," *Renew. Sustain. Energy Rev.*, vol. 99, pp. 159–168, Jan. 2019.

[3] A. Ba, C. O. Ehssein, M. E. M. O. M. Mahmoud, O. Hamdoun, and A. Elhassen, "Comparative study of different DC/DC power converter for optimal PV system using MPPT (P&O) method," *Appl. Sol. Energy*, vol. 54, no. 4, pp. 235–245, Jul. 2018.

[4] K. Vijayan, S. P. Vijayachamundeeswari, K. Sivaperuman, N. Ahsan, T. Logu, and Y. Okada, "A review on advancements, challenges, and prospective of copper and non-copper based thin-film solar cells using facile spray pyrolysis technique," *Sol. Energy*, vol. 234, pp. 81–102, Mar. 2022.

[5] M. A. Soliman, A. Al-Durra, and H. M. Hasanien, "Electrical parameters identification of three-diode photovoltaic model based on equilibrium optimizer algorithm," *IEEE Access*, vol. 9, pp. 41891–41901, 2021.

[6] A. Ali, K. Irshad, M. F. Khan, M. M. Hossain, I. N. A. Al-Duais, and M. Z. Malik, "Artificial intelligence and bio-inspired soft computing-based maximum power plant tracking for a solar photovoltaic system under non-uniform solar irradiance shading conditions—A review," *Sustainability*, vol. 13, no. 19, p. 10575, Sep. 2021.

[7] V. Bhan, S. A. Shaikh, Z. H. Khand, T. Ahmed, L. A. Khan, F. A. Chachar, and A. M. Shaikh, "Performance evaluation of perturb and observe algorithm for MPPT with buck–boost charge controller in photovoltaic systems," *J. Control, Autom. Electr. Syst.*, vol. 32, no. 6, pp. 1652–1662, Dec. 2021.

[8] M. Aldhaifallah, A.-W.-A. Saif, U. Baroudi, H. Rezk, and A. Mohamed, "Fractional incremental resistance based MPPT for thermoelectric generation systems," in *Proc. 18th Int. Multi-Conf. Syst., Signals Devices (SSD)*, Mar. 2021, pp. 902–907.

[9] C. B. N. Fapi, P. Wira, M. Kamta, H. Tchakounté, and B. Colicchio, "Simulation and dSPACE hardware implementation of an improved fractional short-circuit current MPPT algorithm for photovoltaic system," *Appl. Sol. Energy*, vol. 57, no. 2, pp. 93–106, Mar. 2021.

[10] A. I. M. Ali and H. R. A. Mohamed, "Improved P&O MPPT algorithm with efficient open-circuit voltage estimation for two-stage grid-integrated PV system under realistic solar radiation," *Int. J. Electr. Power Energy Syst.*, vol. 137, May 2022, Art. no. 107805.

[11] S. Mahmud, R. Kini, A. Barchowsky, A. Javaid, and R. Khanna, "A two-level MPPT algorithm in dynamic partial shading condition using ripple correlation control," in *Proc. IEEE Appl. Power Electron. Conf. Expo. (APEC)*, Jun. 2021, pp. 89–96.

[12] C. Aouiti and H. Jallouli, "New feedback control techniques of quaternion fuzzy neural networks with time-varying delay," *Int. J. Robust Nonlinear Control*, vol. 31, no. 7, pp. 2783–2809, May 2021.

[13] M. Naseem, M. A. Husain, A. F. Minai, A. N. Khan, M. Amir, J. D. Kumar, and A. Iqbal, "Assessment of meta-heuristic and classical methods for GMPPT of PV system," *Trans. Electr. Electron. Mater.*, vol. 22, no. 3, pp. 217–234, Jun. 2021.

[14] F. Pellitteri, V. Di Dio, C. Puccio, and R. Miceli, "A model of DC-DC converter with switched-capacitor structure for electric vehicle applications," *Energies*, vol. 15, no. 3, p. 1224, Feb. 2022.

[15] D. Verma, S. Nema, R. Agrawal, Y. Sawle, and A. Kumar, "A different approach for maximum power point tracking (MPPT) using impedance matching through non-isolated DC-DC converters in solar photovoltaic systems," *Electronics*, vol. 11, no. 7, p. 1053, Mar. 2022.

[16] E. Foray, C. Martin, B. Allard, and P. Bevilacqua, "Design of a high-to-low voltage, low-power, isolated DC/DC converter for EV applications," *IEEE J. Emerg. Sel. Topics Power Electron.*, early access, Jan. 20, 2022, doi: 10.1109/JESTPE.2022.3144281.

[17] C. H. H. Basha, C. Rani, and S. Odofin, "A review on non-isolated inductor coupled DC-DC converter for photovoltaic grid-connected applications," *Int. J. Renew. Energy Res.*, vol. 7, no. 4, pp. 1570–1585, 2017.

[18] A. Goudarzian, A. Khosravi, and H. A. Raeisi, "Modeling, design and control of a modified flyback converter with ability of right-half-plane zero alleviation in continuous conduction mode," *Eng. Sci. Technol., Int. J.*, vol. 26, Feb. 2022, Art. no. 101007.

[19] D. Rong, X. Sun, and N. Wang, "A high step-up interleaved boost-Cuk converter with integrated magnetic coupled inductors," *IET Renew. Power Gener.*, vol. 16, no. 3, pp. 607–621, Feb. 2022.

[20] E. Kim, M. Warner, and I. Bhattacharya, "Adaptive step size incremental conductance based maximum power point tracking (MPPT)," in *Proc. 47th IEEE Photovoltaic Spec. Conf. (PVSC)*, Jun. 2020, pp. 2335–2339.

[21] C. H. Basha and C. Rani, "Different conventional and soft computing MPPT techniques for solar PV systems with high step-up boost converters: A comprehensive analysis," *Energies*, vol. 13, no. 2, p. 371, Jan. 2020.

[22] K. Anoop and M. Nandakumar, "A novel maximum power point tracking method based on particle swarm optimization combined with one cycle control," in *Proc. Int. Conf. Power, Instrum., Control Comput. (PICC)*, Jan. 2018, pp. 1–6.

[23] M. N. Ali, K. Mahmoud, M. Lehtonen, and M. M. F. Darwish, "Promising MPPT methods combining metaheuristic, fuzzy-logic and ANN techniques for grid-connected photovoltaic," *Sensors*, vol. 21, no. 4, p. 1244, Feb. 2021.

[24] C. H. H. Basha and C. Rani, "Performance analysis of MPPT techniques for dynamic irradiation condition of solar PV," *Int. J. Fuzzy Syst.*, vol. 22, no. 8, pp. 2577–2598, Nov. 2020.

[25] A. B. R. Ram, T. S. Sirish, M. V. S. Kumar, and A. S. S. R. Murthy, "Comparison of incremental conductance with fuzzy controller for a PLL-less scheme for grid-interfaced PV system," in *Microelectronics, Electromagnetics and Telecommunications*. Singapore: Springer, 2021, pp. 579–589.

[26] U. Yilmaz, A. Kircay, and S. Borekci, "PV system fuzzy logic MPPT method and PI control as a charge controller," *Renew. Sustain. Energy Rev.*, vol. 81, pp. 994–1001, Jan. 2018.

[27] K. Loukil, H. Abbes, H. Abid, M. Abid, and A. Toumi, "Design and implementation of reconfigurable MPPT fuzzy controller for photovoltaic systems," *Ain Shams Eng. J.*, vol. 11, no. 2, pp. 319–328, Jun. 2020.

[28] A. Ali, K. Almutairi, M. Z. Malik, K. Irshad, V. Tirth, S. Algarni, M. H. Zahir, S. Islam, M. Shafiullah, and N. K. Shukla, "Review of online and soft computing maximum power point tracking techniques under non-uniform solar irradiation conditions," *Energies*, vol. 13, no. 12, p. 3256, Jun. 2020.

[29] C. H. Basha and M. Murali, "A new design of transformerless, non-isolated, high step-up DC-DC converter with hybrid fuzzy logic MPPT controller," *Int. J. Circuit Theory Appl.*, vol. 50, no. 1, pp. 272–297, Jan. 2022.

[30] J. Reynolds, Y. Rezgui, A. Kwan, and S. Piriou, "A zone-level, building energy optimisation combining an artificial neural network, a genetic algorithm, and model predictive control," *Energy*, vol. 151, pp. 729–739, May 2018.

[31] R. B. Bollipo, S. Mikkili, and P. K. Bonthagorla, "Critical review on PV MPPT techniques: Classical, intelligent and optimisation," *IET Renew. Power Gener.*, vol. 14, no. 9, pp. 1433–1452, 2020.

[32] C. H. Basha, M. Murali, S. Rafikiran, T. Mariprasath, and M. B. Reddy, "An improved differential evolution optimization controller for enhancing the performance of PEM fuel cell powered electric vehicle system," *Mater. Today, Proc.*, vol. 52, pp. 308–314, Jan. 2022.

[33] M. Murali, "Performance analysis of different types of solar photovoltaic cell techniques using MATLAB/simulink," in *Proc. 4th Int. Conf. Inventive Mater. Sci. Appl.* Singapore: Springer, 2022, pp. 203–215.

[34] C. G. Villegas-Mier, J. Rodriguez-Resendiz, J. M. Álvarez-Alvarado, H. Rodriguez-Resendiz, A. M. Herrera-Navarro, and O. Rodríguez-Abreo, "Artificial neural networks in MPPT algorithms for optimization of photovoltaic power systems: A review," *Micromachines*, vol. 12, no. 10, p. 1260, Oct. 2021.

[35] S.-C. Wang, H.-Y. Pai, G.-J. Chen, and Y.-H. Liu, "A fast and efficient maximum power tracking combining simplified state estimation with adaptive perturb and observe," *IEEE Access*, vol. 8, pp. 155319–155328, 2020.
[36] B. Karthikeyan, D. Karthikeyan, V. P. Arumbu, K. Sundararaju, R. Palanisamy, and P. Divya, "A feed-forward neural network based MPPT controller for PEMFC system with ultra high step up converter," in *Proc. Int. Conf. Power Electron. Renew. Energy Syst.* Singapore: Springer, 2022, pp. 247–255.
[37] P. K. Nkounhawa, D. Ndapeu, and B. Kenmeugne, "Artificial neural network (ANN) and adaptive neuro-fuzzy inference system (ANFIS): Application for a photovoltaic system under unstable environmental conditions," *Int. J. Energy Environ. Eng.*, pp. 1–9, 2022, doi: 10.1007/s40095-022-00472-x.
[38] S. Touil, N. Boudjerda, A. Boubakir, and K. E. K. Drissi, "A sliding mode control and artificial neural network based MPPT for a direct grid-connected photovoltaic source," *Asian J. Control*, vol. 21, no. 4, pp. 1892–1905, Jul. 2019.
[39] Z. M. Ali, T. Alquthami, S. Alkhalaf, H. Norouzi, S. Dadfar, and K. Suzuki, "Novel hybrid improved bat algorithm and fuzzy system based MPPT for photovoltaic under variable atmospheric conditions," *Sustain. Energy Technol. Assessments*, vol. 52, Aug. 2022, Art. no. 102156.
[40] M. Badar, I. Ahmad, A. A. Mir, S. Ahmed, and A. Waqas, "An autonomous hybrid DC microgrid with ANN-fuzzy and adaptive terminal sliding mode multi-level control structure," *Control Eng. Pract.*, vol. 121, Apr. 2022, Art. no. 105036.

SHAIK RAFI KIRAN received the master's degree from JNTUH and the Ph.D. degree from JNT University, Anantapur. Currently, he is a Professor and the HOD with the EEE Department, Sri Venkateshwara College of Engineering, Tirupati. He is a Ratified Professor and a Supervisor from JNTUA. He has over 21 years of teaching experience and published more than 40 papers in international and national journals. His research interests include systems identification, control systems, power systems, and power electronics.

C. H. HUSSAIAN BASHA received the bachelor's degree in electrical and electronics engineering from Jawaharlal Nehru Technological University Hyderabad, Anantapur, India, and the master's degree in power electronics and drives from VIT University, India, in 2013 and 2016, respectively. He is working as an Assistant Professor with the Department of EEE, Nanasaheb Mahadik College of Engineering, Peth, Maharashtra, India. He has published various SCI and SCOPUS indexed journals. His research interests include PV cell modeling, fuel cell modeling, soft computing, artificial intelligence, power point tracking techniques, liquid dielectrics, spectroscopy analysis, and design of high step-up DC–DC converters for electric vehicle application.

VISHWA PRATAP SINGH received the Bachelor of Technology degree from UPTU, Lucknow, the Master of Technology degree in information technology and management from the Indian Institute of Information Technology, and the Ph.D. degree from USICT, GGSIPU, Delhi. He has four years of teaching experience. He is working as an Assistant Professor with the Department of CSE, Nanasaheb Mahadik College of Engineering, Peth, Maharashtra, India. His main research work focuses on information security (systems penetration testing), information centric networking, NDN, future internet architectures, and networks security.

C. DHANAMJAYULU (Senior Member, IEEE) received the B.Tech. degree in electronics and communication engineering from JNTU University, Hyderabad, India, the M.Tech. degree in control and instrumentation systems from the Indian Institute of Technology Madras, Chennai, India, and the Ph.D. degree in power electronics from the Vellore Institute of Technology, Vellore, India. He was a Postdoctoral Fellow with the Department of Energy Technology, Aalborg University, Esbjerg, Denmark, from October 2019 to January 2021. He was invited as a Visiting Researcher with the Department of Energy Technology, Aalborg University, funded by the Danida Mobility Grant, Ministry of Foreign Affairs of Denmark, on Denmark's International Development Cooperation. He is currently a Faculty Member and a member of the Control and Automation Department, School of Electrical Engineering, Vellore Institute of Technology, where he has been a Senior Assistant Professor, since 2010. His research interests include multilevel inverters, power converters, active power filters, power quality, grid-connected systems, smart grid, electric vehicle, electric spring, and tuning of memory elements and controller parameters using soft-switching techniques for power converters, average modeling, steady-state modeling, and small-signal modeling stability analysis of the converters and inverters. He is the Academic Editor for the journal *International Transactions on Electrical Energy Systems* (Wiley-Hindawi).

B. RAJANARAYAN PRUSTY (Senior Member, IEEE) received the Ph.D. degree from the National Institute of Technology Karnataka (NITK), Surathkal. He is currently working as an Assistant Professor (Sr. Grade) with the School of Electrical Engineering, Vellore Institute of Technology (VIT), Vellore. He has 15 SCI journal publications and 35 conference publications to his credit. He has authored six book chapters published in CRC press, Elsevier, and Springer. He has coauthored a textbook titled *Power System Analysis: Operation and Control* (I. K. International Publishing House). He has also edited a book titled *Renewable Energy Integration to the Grid: A Probabilistic Perspective* (CRC Press, and Taylor and Francis Books India). He has been an active reviewer, since 2015, and has reviewed 200 manuscripts submitted to repute SCI-indexed journals/conferences. His research interests include time series preprocessing and forecasting, high-dimensional dependence modeling, and probabilistic power systems analysis. His exceptional research work during his Ph.D. degree has led him to crown the prestigious POSOCO Power System Awards (PPSA) for 2019 under the doctoral category by Power System Operation Corporation Ltd. in partnership with FITT, IIT Delhi. In recognition of his research publications, from 2017 to 2019, he was awarded the University Foundation Day Research Award-2019 from BPUT, Odisha. Currently, he is the Associate Editor of *Journal of Electrical Engineering and Technology* (Springer). He is also the Academic Editor of the journals *Mathematical Problems in Engineering* (Hindawi) and *International Transactions on Electrical Energy Systems* (Wiley-Hindawi).

BASEEM KHAN (Senior Member, IEEE) received the B.Eng. degree in electrical engineering from Rajiv Gandhi Technological University, Bhopal, India, in 2008, and the M.Tech. and D.Phil. degrees in electrical engineering from the Maulana Azad National Institute of Technology, Bhopal, in 2010 and 2014, respectively. He is currently working as a Faculty Member of Hawassa University, Ethiopia. His research interests include power systems restructuring, power systems planning, smart grid technologies, meta-heuristic optimization techniques, reliability analysis of renewable energy systems, power quality analysis, and renewable energy integration.